

Modeling Sky Luminance Angular Distribution for Real Sky Conditions: Experimental Evaluation of Existing Algorithms

R. Perez, J. Michalsky, and R. Seals

Introduction

Skylight and direct sunlight are the two components of natural light. The former is an extended source of spatially varied intensity, while the latter can be regarded as a point source. Recently developed daylighting simulation tools can accurately model light penetration within complex structures¹ and effectively complement the time-consuming and expensive scale model approach, if provided with a proper description of these two light sources.

This paper is concerned with skylight. A recent paper by the authors² dealt with the direct sunlight component. A proper description of the skylight source entails a knowledge of the angular distribution of sky luminance. Standard models concerned with integrated diffuse illuminance impinging on a tilted plane³ are insufficient.

Many spatially continuous luminance distribution models have been proposed. In particular, note the CIE standard clear, intermediate, and overcast skies.^{3,4,5} In this paper, we are concerned with models designed to account for changing light intensity distribution as a function of all insolation conditions from overcast through partially cloudy to clear.

Methods

The experimental database

Models are evaluated against an experimental set of data that includes more than 16,000 all-sky scans recorded in Berkeley, CA, between June 1985 and December 1986. Each scan by Lawrence Berkeley Laboratories comprises 186 luminance measurements. Measurements were performed using a multi-purpose scanning photometer developed by Battelle, Pacific Northwest Laboratories, and well suited to the current research application.⁶ In addition to sky scans, we also have time-coincident direct illuminance measurements.

Unfortunately, no time coincident irradiance measurements are available; however, the use of both direct illuminance and diffuse illuminance (through sky scan integration) allows us to adequately describe insolation conditions and to model the correspond-

ing direct and diffuse irradiance.²

The Luminance Distribution Algorithms

We selected six algorithms that are capable of modeling the variations of sky luminance distribution as a function of all insolation conditions. Before describing each algorithm, it is important to remark that each is independent from the data set.

*Brunger algorithm*⁷—The Brunger algorithm was designed to model radiance rather than luminance distribution, hence it may be at a disadvantage in the present evaluation. It uses global and diffuse irradiance as input and parameterizes insolation conditions as a two-dimensional space defined by the ratio of global to extraterrestrial irradiance (i.e., clearness index, k) and the ratio of diffuse to global irradiance, k_d . The geometrical framework of the model is that originally proposed by Hooper, et al.⁸ The governing equation as adapted for luminance distribution is provided in the **Appendix**.

*Harrison algorithm*⁹—This model uses two luminance distribution profiles: overcast and clear sky, respectively L_{oc} and L_{cc} . The general profile is a linear combination of the two, based upon opaque cloud cover. The analytical expression for each profile is provided in the **Appendix**.

Unfortunately, opaque cloud cover data were not available for Berkeley. We did try data obtained in San Francisco, CA, located 30 km away, but results were not encouraging. Much better performance was obtained by estimating the needed input from available data; as a consequence, this model may also be at a disadvantage in the present comparison. After having tried several cloud cover algorithms,¹⁰ the best results were obtained by substituting k to opaque cloud cover.

*Kittler homogeneous sky algorithm*¹¹—This physically based model was developed to calculate both absolute and relative sky patterns for varying insolation conditions parameterized using the illumination turbidity coefficient, T_{ij} .¹² Illumination turbidity may be derived from our direct illuminance data as shown in the **Appendix**, along with the model governing equations.

Note that we use an average luminance value for the model's normalizing constant C_0 . This does not influence the results of the present evaluation because all models are compared in relative terms after

Authors' affiliation: Atmospheric Sciences Research Center, The University at Albany, State University of New York, Albany, NY.

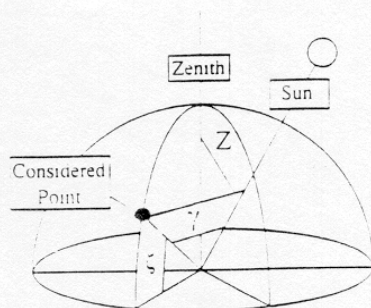


Figure 1—Illustration of the celestial angles used in the paper:

γ is the sun's incidence or scattering angle;
 ϕ is the considered point's elevation; and
 Z is the solar zenith angle

normalization to horizontal diffuse illuminance. (Rule 2 below).

Matsuura Algorithm¹⁴—This model is based on the three CIE standard skies overcast, intermediate, and clear.^{3,4,5} The all-weather distribution is obtained by linear combinations of the intermediate, the overcast, and the clear sky standard models, based on the illuminance cloud ratio, k_c , which is used to parameterize insolation conditions. (k_c is the illuminance equivalent of k .) The model's governing equation is provided in the **Appendix**.

Note that the author provides specific formulae to estimate the zenith luminance input to each of the CIE skies. In the present case, we used measured zenith luminance. Moreover, since all models are normalized to horizontal diffuse illuminance (as in Rule 2 below), the value of the zenith luminance input has no influence on our evaluation.

Perraudéau model¹⁴—This model uses a unique formulae relating sky luminance to diffuse irradiance, with adjustable coefficients depending on insolation conditions. Five sets of coefficients are provided for insolation conditions from overcast to clear as parameterized by a cloud index, N_p , defined as $(1-k)/(1-k_c)$, where k_c is the theoretical clear day value of k . The coefficients were derived experimentally from luminance measurements at five points in the sky. The governing equation is given in the **Appendix**.

ASRC CIE-combination algorithm²—As for the Matsuura algorithm, this model is based on the three CIE skies plus a high turbidity formulation of the CIE clear sky.⁹ The general distribution is obtained via interpolation involving two quantities: sky clearness, ϵ , and sky brightness, Δ . The two parameters may be derived from direct (or global) and diffuse irradiance as shown in the appendix. The interpolation scheme is based on another model that we developed to compute diffuse illuminance on a tilt.² This scheme has been slightly modified since the preliminary algorithm² by developing a more straightforward

relationship between the illuminance model's coefficients and the CIE skies.

The ground rules for model comparison

Rule 1—The input to each model consists of global and direct (diffuse) irradiance. This is consistent with the goal of the daylighting community to exploit irradiance data to derive daylight quantities. Models that use illuminance as input (e.g., Kittler) are not at a disadvantage here, since irradiance and illuminance are linked by a deterministic luminous efficacy.² In fact, these models may even have a slight advantage, since illuminance is the measured quantity while irradiance is modeled. Only the Harrison model requiring opaque cloud cover as input is at a disadvantage.

Rule 2—We are interested in each model's ability to account for the relative angular distribution of luminance in the sky, not its ability to provide absolute luminance values. This is because given a relative profile, one can always obtain the absolute values if either of the following is known: the luminance at any given point in the sky or the integrated diffuse illuminance on any given plane. Both may be obtained in a more straightforward manner from irradiance input than luminance distribution. For the present, we will compare algorithms after having normalized their output to horizontal diffuse illuminance.

Results

Overall results are presented in **Table 1**. The table includes model mean bias (MBE) and root mean square error (RMSE) for all events (16,000 scans, three million data points) in the entire sky dome divided into five regions: the zenith region (60-degree elevation and greater) and three regions below 60-degrees elevation in azimuthal directions facing the sun, opposite the sun, and east-west of the sun. Note that the bias error in the zenithal region is a measure of each model's ability to relate zenith luminance and diffuse illuminance on the horizontal.

Ideal model benchmark—**Table 1** also includes the results of an "ideal" model. This model consists of the mean skylight distributions assembled from the experimental database for each of 750 insolation condition bins defined by the sky clearness, ϵ , the sky brightness, Δ , and the solar zenith angle, Z . This crude, data-dependent model features more than 10,000 empirical coefficients (186 positions in the sky vault times 750 bins). It is not intended for use as a working model, but rather as a benchmark to estimate how much dispersion remains (RMSE) even when unbiased, insolation-dependent luminance distributions are used. In effect, this model shows the limit of accuracy achievable with the type of all-weather model considered here. The remaining RMSE would be

Table 1—Mean sky luminance (cd/m²), model mean bias, and root mean square errors as a function of sky condition and position in the sky

	Entire sky		Zenithal region		Sun-facing region		E/W-of-sun region		North-of-sun region	
All conditions	4478		4294		8377		4003		3446	
Mean luminance (15929 scans)	MBE	RMSE	MBE	RMSE	MBE	RMSE	MBE	RMSE	MBE	RMSE
Ideal	0	1880	0	1768	1	3319	1	1264	0	1079
ASRC-CIE	-75	2113	87	1920	-10	3776	-42	1396	-361	1250
Brunger	227	2312	207	2092	-489	4157	-268	1511	-333	1344
Harrison	197	2363	283	2045	-1063	4324	-195	1522	109	1356
Matsuura	161	2443	267	2255	-1058	4451	-27	1489	-46	1426
Kittler	229	2520	461	2350	-1373	4536	-165	1552	-6	1552
Perraudeau	26	2553	-250	2238	36	4097	111	1913	112	2147
Bright overcast conditions	12067		14238		18393		10244		7954	
Mean luminance (685 scans)	MBE	RMSE	MBE	RMSE	MBE	RMSE	MBE	RMSE	MBE	RMSE
Ideal	0	3721	0	3960	2	6584	0	2212	0	1929
ASRC-CIE	36	3952	193	4038	-499	7018	573	2474	-282	1981
Harrison	57	4382	401	4404	-3195	7772	519	2607	1772	2666
Brunger	-26	4423	534	5009	582	7676	-553	2605	-43	2172
Matsuura	-431	5877	1242	6021	-7319	10660	426	3077	2420	3558
Kittler	-365	5981	954	6085	-7379	10765	591	3176	2736	3829
Perraudeau	161	6144	-1665	5872	-3412	9120	2736	4631	4829	5743
Clear conditions	3808		3040		7155		3199		2757	
Mean luminance (4803 scans)	MBE	RMSE	MBE	RMSE	MBE	RMSE	MBE	RMSE	MBE	RMSE
Ideal	0	773	0	741	0	1307	0	543	0	472
ASRC-CIE	-101	1051	-23	1135	100	1736	-125	681	-310	713
Matsuura	-102	1051	-23	1135	95	1736	-125	681	-312	715
Kittler	-252	1163	450	1196	-394	1833	-383	849	-534	860
Harrison	-300	1334	261	1014	-664	2374	-441	1013	-224	726
Brunger	-275	1350	96	1072	-394	2442	-310	887	-453	910
Perraudeau	-340	1434	121	1032	393	2175	-579	1182	-965	1390
Dark overcast conditions	1114		1313		1109		1055		1043	
Mean luminance (787 scans)	MBE	RMSE	MBE	RMSE	MBE	RMSE	MBE	RMSE	MBE	RMSE
Ideal	0	497	0	557	1	670	0	469	0	484
Brunger	-24	527	42	377	-87	717	-28	496	-25	507
Matsuura	-59	554	108	402	-146	752	-88	523	-88	533
ASRC-CIE	-59	554	108	402	-146	752	-88	523	-88	533
Kittler	-59	555	109	403	-147	752	-88	523	-89	533
Perraudeau	95	586	-180	438	243	773	139	555	148	574
Harrison	15	596	-45	457	356	888	-40	513	-122	545

mostly attributable to one-of-kind random cloud/haze patterns that the present models cannot address.

Table 1 also illustrates model behavior for three specific insolation conditions: clear sky conditions, bright overcast, and dark overcast. In each case, models have been ranked with respect to their overall RMS error. The validation results reported in **Table 1** include all solar elevations; it is interesting to note that the ranking of the models and their relative error do not change appreciably with solar elevation.

These results are graphically illustrated in **Figure 2**, where model bias trends throughout the sky dome

may be observed for a specific range of solar elevations (≈ 45 degrees).

Discussion

Results in **Table 1** show that overall the ASRC-CIE combination model exhibits the lowest RMSE in all orientations and a low MBE for all but the direction opposite the sun. The Brunger algorithm comes in second in terms of RMSE with the best performance for dark overcast conditions. This is remarkable since this model was not designed as a luminance distribution model. Following are the Harrison model (remarkable

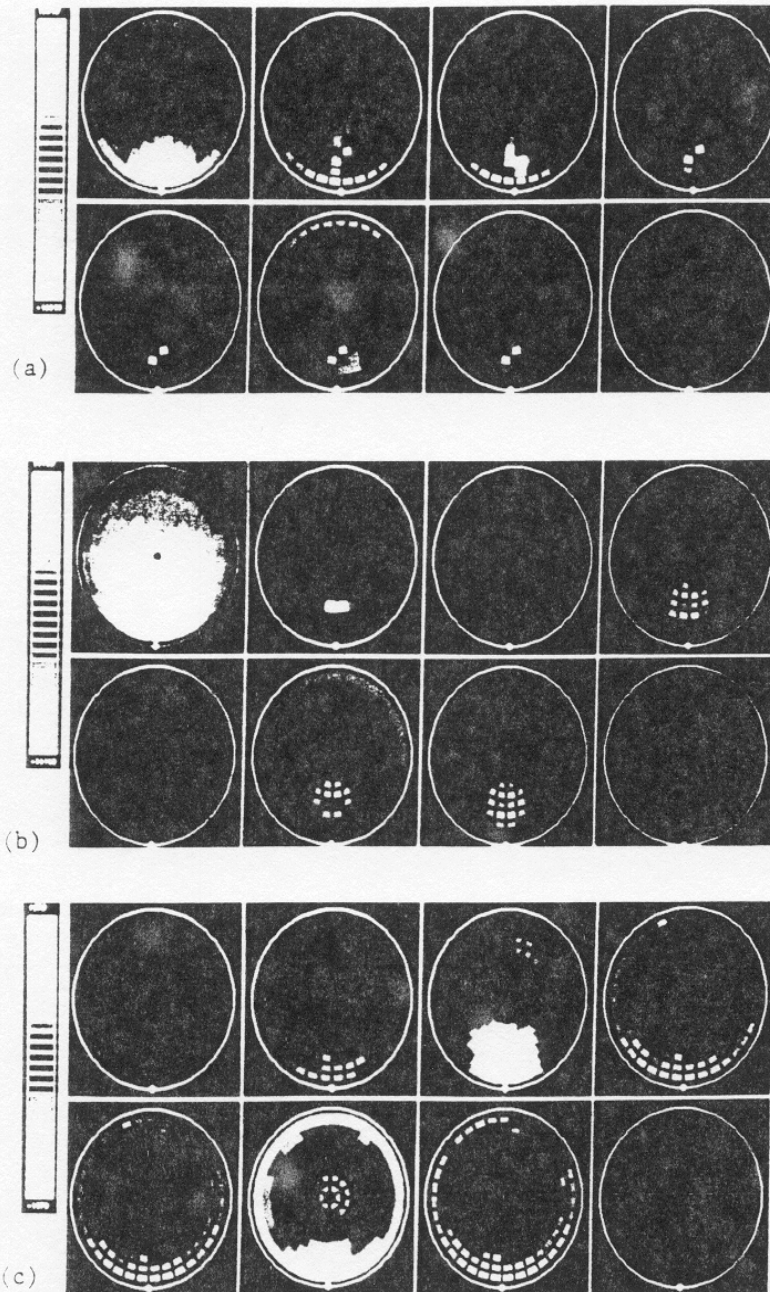


Figure 2—Bias error as a function of sky position for (a) clear skies, (b) bright overcast skies, and (c) dark overcast skies. The top row of each group from left to right displays the observed mean illuminance distribution followed by the bias errors for the Brunger, Harrison, and Kittler models. The bottom row from left to right

displays the bias error of the ASRC, Perraudau, Matsuura, and ideal models. A gray scale indicates the bias magnitude (low bias = black, high bias = white). Continuous areas indicate positive bias and discontinuous areas negative bias.

given the fact that we used a substitute input), the Matsuura, Kittler, and Perraudau algorithms.

It is interesting to note that the two models with the best performance rely on a two-dimensional parameterization of insolation conditions that, in effect, differentiates between the clearness of the sky

(overcast vs. clear) and its brightness (thin vs. thick cloudiness). This would support the thesis that a key factor in the successful modeling of skylight distribution is an adequate parameterization of insolation conditions, as much as the model's geometrical framework. The fact that the Matsuura algorithm,

which uses the same CIE functions as the ASRC algorithm but another parameterization, performs less well, tends to confirm our assertion. Indeed, **Figure 2** and **Table 1** show that the clear sky performance and dark overcast sky performance of the Matsuura algorithm is very similar to that of ASRC, but that the former does not account well for bright overcast skies.

Note that a more versatile parameterization does not necessarily mean more input quantities. In fact, all models tested here use exactly the same input information.

A similar observation is made for the Kittler model which performs similarly to the ASRC and Matsuura algorithms for the extreme conditions, but does not handle the intermediate cases well. The probable reason is that the turbidity parameter ceases to be appropriate as soon as skies become inhomogeneous (i.e., partly cloudy).

The main source of weakness using the Perraudau algorithm may be the fact that this was experimentally derived from only a limited number of points in the sky dome, leading to possible distortions in other directions. The large RMSEs in the directions perpendicular and opposite to the sun are symptomatic of this.

Finally, it is very important to remark that the ideal model performance, exemplified by the mean sky model, is not considerably better than the best algorithms tested here, although possibilities for systematic improvement exist as seen from the well defined bias patterns. Also, the ideal model RMSE remains significant because of the random nature of clouds superimposed on the mean skylight distribution background. With support from the US National Science Foundation we are in the process of developing an algorithm that will account for this random effect.

Conclusions

Our study illustrates some basic weaknesses and strengths of existing methods to model the distribution of skylight from irradiance data for real sky conditions. The best algorithms tested here, the ASRC-CIE² and Brunger⁷ models, come close to the precision achievable by this type of model although room for systematic performance improvement does exist. We also note that the random nature of clouds, while having little impact on average skylight distribution, accounts for much short-term uncertainty, particularly in the vicinity of the sun.

The reader may want to use the results of this validation to select a model that extrapolates sky luminance spatial distribution from routine irradiance data. It must be remembered that the validation is site specific and will have to be repeated when

data become available. On the other hand, to the credit of this study, it must be said that the Berkeley data feature a wide range of insolation conditions from dark overcast to very clear; that it has been shown that site dependency is not a major issue if insolation conditions are properly parameterized; and that the present test is fully independent.

Acknowledgements

This work is supported by the U.S. National Science Foundation under grant MSM 8915165. Thanks to A. Zelenka for his suggestions on cloud cover.

References

1. Fontoynt, M.R. 1987. Simulation of complex window components using ray-tracing simulation. *ISES Solar World Congress*.
2. Perez, R.; Ineichen, P.; Seals, R.; Michalsky, J.; and Stewart, R. 1990. Modeling daylight availability and irradiance components. *Solar Energy* 44:271-289.
3. Commission Internationale de l'Eclairage. 1973. *Standardization of luminous distribution on clear skies*. CIE Publication No. 22. Paris: CIE.
4. Moon, P. and Spencer, D., 1942. Illumination from a nonuniform sky. *Illum Eng* 37:707-726.
5. Matsuura, K. 1987. Luminance distributions of various reference skies. *CIE technical report of TC 3-09* (draft).
6. Kleckner, E.W.; Michalsky, J.J.; et al. 1981. *A multi-purpose computer controlled scanning photometer* PNL-4081. Richland, WA: Pacific Northwest Laboratory.
7. Brunger, A.P. 1987. The magnitude, variability, and angular characteristics of the shortwave sky radiance at Toronto. University of Toronto Ph.D. thesis.
8. Hooper, F.C. and Brunger, A.P., 1980. A model for the angular distribution of sky radiance. *J. Solar Energy Engineering* 102:196-202.
9. Harrison, A. W. 1992. Directional luminance versus cloud cover and solar position. *Solar Energy* 46:13-20.
10. Kasten, F. and Czeplak, G. 1980. Solar and terrestrial radiation dependent on the amount and type of cloud. *Solar Energy* 34: 177-189.
11. Kittler, R. 1986. Luminance models of homogeneous skies for design and energy performance predictions. *Proc. 2nd International Daylighting Conference*. Atlanta, GA: American Society of Heating, Refrigerating and Air-Conditioning Engineers.
12. Navvab, M., Karayel, M., Ne'eman, E., and Selkowitz, S. 1984. Analysis of turbidity for daylight calculations. *Energy and Buildings*. 6:293-303.
13. Matsuura, K. and Iwata, T. 1990. A model of daylight source for the daylight illuminance calculations on the all weather conditions. *Proc. 3rd Int. Daylighting Conference*, edited by A. Spiridonov.

14. Perraudeau, M. 1988. Luminance models. *National lighting conference and daylighting colloquium*, Cambridge, England: Robinson College.
15. U. S. National Science Foundation. Research Project # MSM8915165.

Nomenclature

A	normal illuminance from any sky element, normalized to E_{v_0}
ac, ai, aov	weighting factors used in Matsuura model
ao, ai, a2, a3	coefficients for Brunger's model
B	normal direct illuminance, normalized to E_{v_0}
bc, bct, bl and bo	coefficients used in ASRC-CIE model
C	opaque cloud cover
C_0	normalizing luminance constant used in Kittler model
d1, e1, f1, d2, e2, d3, e3, f3	coefficients used in Perraudeau model
E_{hd}	horizontal diffuse irradiance
E_{eo}	direct normal extraterrestrial irradiance
E_{esn}	direct normal irradiance
E_{vd}	diffuse illuminance on the horizontal
E_{vo}	direct normal extraterrestrial illuminance
E_{vsn}	direct normal illuminance
$f'(\gamma)$	function of solar incidence used in Perraudeau model
f	modeling function of the relative diffuse indicatrix (Kittler)
$g'(\phi)$	function of points elevation used in Perraudeau model
G	zenithal gradation function used in Kittler model
G_r	ground reflectance (Kittler)
$h'(Z)$	function of solar zenith angle used in Perraudeau model
k	ratio of diffuse to global irradiance
K_s	solar air mass expression (Makhotkin) used in Kittler model
k_t	clearness index (ratio of global to extraterrestrial irradiance)
k_v	ratio of diffuse to global illuminance
$L_{vc-cie-c}$	luminance at considered point using CIE standard clear sky
$L_{vc-cie-ct}$	luminance at considered point from CIE clear-turbid expression
$L_{vc-cie-i}$	luminance at considered point from CIE intermediate sky
$L_{vc-cie-o}$	luminance at considered point from CIE overcast sky
L_{vc}	luminance at considered point
L_{vcc}	clear-sky luminance at considered point in Harrison model

L_{vco}	overcast luminance at considered point in Harrison's model
M	function of T_{ij} modulating f (Kittler model)
m	sun's air mass
N	function of T_{ij} modulating f (Kittler model)
N_p	cloud index used in Perraudeau model
P_a	air mass of considered point in Kittler model (Makhotkin) ¹¹
P_{aii}	extinction coefficient for the considered sky element in Kittler model
R_{zo}	function of Z and B used in Kittler model
S_{aii}	extinction coefficient in the direction of the sun (Kittler model)
T_{ij}	illumination turbidity coefficient
X_1	forward elongation of diffusion indicatrix (Kittler model)
Z	solar zenith angle
Z_f	function of T_{ij} , G_r and X_1 used in Kittler model
γ	angle between the direction of the sun and the considered point
Δ	sky brightness used in ASRC-CIE model
ϵ	sky clearness used in ASRC-CIE model
ϕ	angular elevation of considered point in the sky

Appendix: Model-governing equations

Brunger's model

$$L_c = E_{vd} \{ [a_0 + a_1 \sin \phi + a_2 \exp(-a_3 \gamma)] / [\pi(a_0 + 2a_1/3) + 2a_2 I(Z, a_3)] \} \quad (1)$$

where L_c is the luminance at the considered point in the sky dome.

E_{vd} is the horizontal diffuse illuminance.

ϕ is the angular elevation of the considered point. γ is the angle between the considered point and the sun's position.

Z is the solar zenith angle (all angles are illustrated in **Figure 1**).

a_0 , a_1 , a_2 , and a_3 are four experimentally derived coefficients, function of k, and k (each function is discrete and consists of a 9-by-9 k_t -by- k matrix,⁷ and

$I(Z, a_3)$ is a normalizing function equal to

$$I_1 (\pi - I_4 (1 - I_2/I_3)) \quad (2)$$

$$\text{with } I_1 = [1 + \exp(-a_3 \pi/2)] / [a_3^2 + 4] \quad (3)$$

$$I_2 = 2[1 - \exp(-a_3 \pi)] \quad (4)$$

$$I_3 = \pi a_3 [1 + \exp(-a_3 \pi/2)] \quad (5)$$

Coefficients for the Brunger model:

k_t	0.5	0.15	0.25	0.35	0.45	0.55	0.65	0.75	0.85
0.95	0.1864	0.2002	0.1380	0.1508	0.1718	0.2060	0.1605	0.1482	0.1505
0.85	0.1431	0.2303	0.3477	0.2664	0.2139	0.1520	0.1151	0.1358	0.1529
0.75	0.2213	0.2995	0.3687	0.2684	0.201	0.1870	0.1842	0.1566	0.1700
0.65	0.2818	0.3423	0.3851	0.2843	0.2713	0.1597	0.2088	0.1273	0.1834
0.55	0.3784	0.4751	0.6079	0.2892	0.2816	0.2465	0.207	0.2477	0.2396
0.45	0.4132	0.4479	0.4208	0.2337	0.2822	0.2916	0.2583	0.2457	0.2315
0.35	0.4055	0.3979	0.3478	0.2749	0.3162	0.3006	0.2871	0.2491	0.2510
0.25	0.3834	0.3614	0.3249	0.3019	0.3289	0.3417	0.3153	0.3071	0.2971
0.15	0.3624	0.3414	0.3214	0.3179	0.3339	0.3388	0.336	0.3243	0.3061

a_1

0.95	0.1979	0.1772	0.093	0.5472	0.0566	-0.0294	0.0755	0.1579	0.16494
0.85	0.142	0.0346	-0.215	-0.159	0.307	0.1497	0.1805	0.2404	0.17190
0.75	0.0064	-0.129	-0.292	-0.1615	-0.1275	-0.0632	0.0253	0.3003	0.10341
0.65	-0.097	-0.200	-0.272	-0.1645	-0.1837	-0.1715	-0.052	-0.05	-0.0934
0.55	-0.219	-0.342	-0.483	-0.1953	-0.1945	-0.1245	-0.0927	-0.0711	-0.1369
0.45	-0.268	-0.317	-0.292	-0.1015	-0.1842	-0.2065	-0.1654	-0.1398	-0.2028
0.35	-0.269	-0.270	-0.222	-0.152	-0.2039	-0.2172	-0.2184	-0.2224	-0.0907
0.25	-0.253	-0.238	-0.207	-0.191	-0.230	-0.2574	-0.2338	-0.2576	-0.3126
0.15	-0.239	-0.225	-0.212	-0.218	-0.244	-0.258	-0.26	-0.3003	-0.4531

a_2

0.95	0	0	0.289	0.6659	0.8734	2.9511	2.5897	2.3141	2.09639
0.85	2.636	2.651	5.317	1.7758	1.6099	1.8315	2.2284	2.0385	1.87865
0.75	2.6374	2.6389	2.6268	4.5224	1.4096	1.2819	1.308	1.8486	1.71881
0.65	3.0275	3.4175	4.1962	5.296	2.822	1.2964	1.3225	1.5961	1.58902
0.55	5.1376	7.2477	11.078	2.1346	3.8606	2.9163	1.1098	1.5836	1.58195
0.45	7.2395	9.3413	11.435	11.792	6.03	2.7327	1.9525	1.512	1.5803
0.35	8.5103	9.7812	10.221	9.0073	6.2226	4.5443	2.6467	1.5992	0.9733
0.25	8.8665	9.2227	8.6642	7.1072	5.2072	4.1918	3.886	2.3127	1.3594
0.15	8.5607	8.2550	7.2873	5.9104	4.7135	4.2199	4.2481	1.9157	1.612

a_3

0.95	1	1	0.9667	1.6755	2.4129	3.7221	3.9387	6.6941	7.86410
0.85	5.525	3.6487	4.4211	2.859	3.726	4.6125	4.1553	9.4496	9.03404
0.75	4.385	3.245	2.8413	4.0842	2.2453	2.5932	3.1127	14.744	8.61843
0.65	4.3185	4.252	5.259	4.3678	3.486	1.9183	2.8364	2.0993	2.49287
0.55	4.3692	4.42	4.588	3.7268	3.7447	4.076	2.5586	3.45	2.88645
0.45	4.5343	4.6994	4.9789	5.3698	4.5241	3.7624	3.3769	2.964	2.3229
0.35	4.7686	5.0028	5.3062	5.6336	5.8975	4.266	3.594	2.6404	2.6775
0.25	4.9699	5.1712	5.3395	5.3729	5.1121	4.3268	4.392	3.5189	2.397
0.15	5.0767	5.1834	5.1957	5.0519	4.7309	4.3497	4.3727	3.268	2.319

Coefficients for Perradeau model:

N_p	d_1	e_1	f_1	d_2	e_2	d_3	e_3	f_3
0.00 - 0.05	32.33	13.16	3.24	1.18	0.23	0.76	0.13	0.2
0.05 - 0.20	17.82	23.99	13.35	1.7	0.89	0.45	0.1	0.59
0.20 - 0.70	14.41	69.7	10.18	2.03	1.31	0.83	-0.29	0.38
0.70 - 0.90	13.05	124.96	7.49	2.21	1.54	0.83	-0.28	0.42
0.90 - 1.00	12.89	243.28	3.26	2.25	1.59	1.04	-0.41	0.2

$$I_4 = 2Z \sin Z - 0.02\pi \sin(2Z) \quad (6) \quad M = 0.71/T_{ii}^{0.5} \quad (23)$$

Harrison's model

$$L_{vcc} = 0.4 + 0.21 Z + 0.27 \sin\phi + 1.45 \exp(-2.41 \gamma) \quad (7) \quad X_1 = 0.115375 N \quad (24)$$

$$L_{vcc} = [1.28 + 147 \exp(-11.1\gamma) + 4.28 \cos^2\gamma \cos Z] * [1 - \exp(-0.42/\sin\phi)] * [1 - \exp(-0.67/\cos Z)] \quad (8) \quad C_o = 7705 \text{ cd/m}^2 \quad (25)$$

The general profile, L_{vc} , is a linear combination of the two, based upon opaque cloud cover, C .

$$L_{vc} = C L_{vco} + (1-C) L_{vcc} \quad (9) \quad \text{where } L_{vc,cie,c} \text{ is the CIE clear sky luminance}^3 \text{ from} \quad (26)$$

Kittler's model

Illuminance turbidity T_{ii} is obtained from

$$T_{ii} = (\ln E_{vo} - \ln E_{vsn}) (9.9 + 0.043m) / m \quad (10)$$

with E_{vo} = direct normal extraterrestrial illuminance

E_{vsn} = direct normal illuminance at the ground

m = sun's air mass

The governing equation of the model is

$$L_{vc} = (C_o/K_s) \{ (G R_{zo}/Z_f) + (A - B)(K_s P_a F - X_1 - 3) / (K_s - P_a) - 2(A + B) \} \quad (11)$$

If the sun's elevation ($\pi/2 - Z$) is equal to the considered point's elevation, the equation becomes

$$L_{vc} = (C_o/K_s) \{ (G R_{zo}/Z_f) + B [0.1 T_{ii}(K_s^2 f - X_1 - 3) - 4] \} \quad (12)$$

$$\text{where } A = \exp(-P_{a1} T_{ii} P_a) \quad (13)$$

$$\text{with } P_{a1} = 1/(9.9 + 0.043 P_a) \quad (14)$$

$$P_a = [(\sin^2\phi + 0.0031465)^{0.5} - \sin\phi] / 0.001572 \quad (15)$$

$$B = \exp(-S_{a1} T_{ii} K_s) \quad (16)$$

$$\text{with } S_{a1} = 1/(9.9 + 0.043 K_s) \quad (17)$$

$$K_s = [(\cos^2 Z + 0.0031465)^{0.5} - \cos Z] / 0.001572 \quad (18)$$

$$G = 0.8 + G_r^3 + 1.64(1 - 0.7G_r^3)\sin\phi + A(1 - G_r)(1 - 1.5\sin\phi) \quad (19)$$

with G_r = ground reflectance (assumed here to be 0.2)

$$R_{zo} = 1 + B + 1.5(1 - B)\cos Z \quad (20)$$

$$f = 1 + N (\exp(-3\gamma) - 0.009) + M \cos^2\gamma \quad (21)$$

$$\text{with } N = 4.3 T_{ii}^{1.9} \exp(-0.35 T_{ii}) \quad (22)$$

Matsuura's model

$$L_{vc} = a_c L_{vc,cie,c} + a_i L_{vc,cie,i} + a_{ov} L_{vc,cie,o} \quad (26)$$

where $L_{vc,cie,c}$ is the CIE clear sky luminance³ from

$L_{vc,cie,i}$ the CIE intermediate sky luminance⁵

$L_{vc,cie,o}$ is the CIE overcast sky luminance⁴

a_c , a_i and a_{ov} are three coefficients depending on k_c as follows

if $k_c < 0.3$

$$a_c = 1 \text{ and } a_i = a_{ov} = 0 \quad (27)$$

if $k_c \geq 0.3$ and $k_c < 0.65$

$$a_c = 1 - (k_c - 0.3)/0.35, a_i = 1 - a_c \text{ and } a_{ov} = 0 \quad (28)$$

if $k_c \geq 0.65$

$$a_c = 0, a_i = 1 - (k_c - 0.65)/0.35, \text{ and } a_{ov} = 1 - a_i \quad (29)$$

Note that the analytical formulations of $L_{vc,cie,c}$, $L_{vc,cie,i}$, and $L_{vc,cie,o}$ are provided by Perez, et al. (1990).²

Perraudeau's model

$$L_{vc} = E_{ed} f(\gamma) g'(\phi) h'(Z) \quad (30)$$

where E_{ed} is the horizontal diffuse irradiance

$$f(\gamma) = d_1 + e_1 \exp(-3\gamma) + f_1 \cos^2 \gamma \quad (31)$$

$$g'(\phi) = d_2 - e_2 (\sin\phi)^{0.6} \quad (32)$$

$$h'(Z) = d_3 + e_3 \cos Z + f_3 \sin Z \quad (33)$$

where d_1 , e_1 , f_1 , d_2 , e_2 , d_3 , e_3 and f_3 are experimentally derived coefficients treated as discrete functions of N_p , defined as $(1-k)/(1-k_o)$, where k_o is the theoretical clear day value of k .

There are five values for each coefficient for conditions ranging from overcast to clear (opposite).

ASRC-CIE model

Determination of sky clearness ϵ and brightness Δ

$$\epsilon = [(E_{ed} + E_{esn})/E_{ed} + 1.041 Z^3] / [1 + 1.041 Z^3] \quad (34)$$

where E_{esn} is the direct normal-incident irradiance, and $\Delta = m E_{ed}/E_{e0}$. (35)

where E_{e0} is the normal-incident extraterrestrial irradiance

The model-governing equation is

$$L_{vc} = b_c L_{vc,cie,c} + b_{ct} L_{vc,cie,ct} - b_i L_{vc,cie,i} + b_o L_{vc,cie,o} \quad (36)$$

where $L_{vc,cie,ct}$ is a high turbidity form of the CIE clear sky.⁷

b_c , b_{ct} , b_i and b_o are coefficients depending on ϵ and Δ as follows

if $\epsilon \leq 1.4$

$$b_i = \max \left(0, \min \{ 1, (\Delta - 0.15)/0.6 + (\epsilon - 1)/0.4 \} \right) \quad (37)$$

$$b_o = 1 - b_i \text{ and } b_c = b_{ct} = 0 \quad (38)$$

if $1.4 < \epsilon \leq 3$

$$b_{ct} = (\epsilon - 1.4)/1.6, b_i = 1 - b_{ct} \text{ and } b_c = b_o = 0 \quad (39)$$

if $\epsilon > 3$

$$b_c = \min[1, (\epsilon - 3)/3], b_{ct} = 1 - b_c \text{ and } b_i = b_o = 0 \quad (40)$$

As above, note that the analytical formulations of $L_{vc,cie,ct}$, $L_{vc,cie,ct}$, $L_{vc,cie,i}$ and $L_{vc,cie,o}$ are provided by Perez.⁷